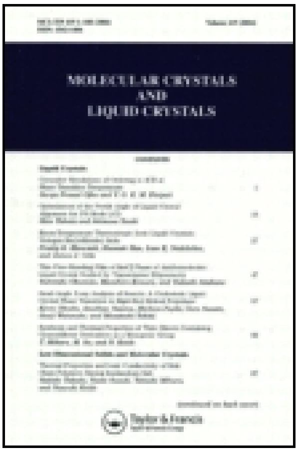

Molecular Crystals and Liquid Crystals
Publication details, including instructions for authors and subscription information:
http://www.tandfonline.com/loi/gmcl20

New-type Phase Transition Coupled with Spin and Charge in Iron Mixed-Valence System

Norimichi Kojima [a] , Miho Itoi [a] , Yuuki Ono [a] , Masashi Ohkubo [a] , Yasuhiro Kobayashi [b] & Makoto Seto [b]

[a] Department of Basic Science, Graduate School of Arts and Sciences, The University of Tokyo, Tokyo, 153-8902, Japan

[b] Research Reactor Institute, Kyoto University, Osaka, 590-0494, Japan

Version of record first published: 18 Oct 2010

To cite this article: Norimichi Kojima, Miho Itoi, Yuuki Ono, Masashi Ohkubo, Yasuhiro Kobayashi & Makoto Seto (2003): New-type Phase Transition Coupled with Spin and Charge in Iron Mixed-Valence System, Molecular Crystals and Liquid Crystals, 379:1, 349-356

To link to this article: http://dx.doi.org/10.1080/713738681

Mol. Cryst. Liq. Cryst., Vol. 379, pp. 349-356
Copyright © 2002 Taylor & Francis
1058-725X/02 $12.00 + .00
DOI: 10.1080/10587250290090714

New-type Phase Transition Coupled with Spin and Charge in Iron Mixed-Valence System

NORIMICHI KOJIMA[a], MIHO ITOI[a], YUUKI ONO[a],
MASASHI OHKUBO[a], YASUHIRO KOBAYASHI[b]
and MAKOTO SETO[b]

[a]*Department of Basic Science, Graduate School of Arts and Sciences, The University of Tokyo, Tokyo 153-8902, Japan and*
[b]*Research Reactor Institute, Kyoto University, Osaka 590-0494, Japan*

We have investigated the physical properties of $(n\text{-}C_nH_{2n+1})_4N[Fe^{II}Fe^{III}(dto)_3]$(dto = $C_2O_2S_2$) by means of ^{57}Fe Mössbauer spectroscopy, magnetic susceptibility, and ESR. From the analysis of ^{57}Fe Mössbauer spectra and ESR signal, we have discovered a new type of first order phase transition around 120 K for $(n\text{-}C_nH_{2n+1})_4N$ $Fe^{II}Fe^{III}(dto)_3]$(n = 3, 4), where the charge transfer transition between Fe^{II} and Fe^{III} occurs reversibly. In the higher temperature phase, the Fe^{III} (S = 1/2) and Fe^{II} (S = 2) sites are coordinated by six S atoms and six O atoms, respectively. In the lower temperature phase, on the other hand, the Fe^{III} (S = 5/2) and Fe^{II} (S = 0) sites are coordinated by six O atoms and six S atoms, respectively. Moreover, we have found the ferromagnetic phase transition in this system. The ferromagnetic order is induced by the charge transfer interaction between the Fe^{III} (S = 5/2) and Fe^{II} (S = 0) sites.

Keywords: spin crossover; ferromagnetism; charge transfer; phase transition; mixed valence

INTRODUCTION

Transition metal complexes with d^4-d^7 configuration have a possibility of spin transition between a low-spin state and a high spin state. The spin crossover phenomenon has recently gained renewed importance since the discovery of the photo-induced spin transition (called LIESST = Light Induced Excited Spin State Trapping) for $[Fe(ptz)_6](BF_4)_2$(ptz = 1-propyltetrazole)[1] and the thermally induced spin crossover transition with large thermal hysteresis around room temperature for a triazole bridged iron(II) complex[2].

In the case of mixed-valence complexes whose spin states are situated in the spin-crossover region, new types of conjugated phenomena coupled with spin and charge are expected. From this viewpoint, we have synthesized new-type of mixed-valence iron complex system, $(n\text{-}C_nH_{2n+1})_4N\ [Fe^{II}Fe^{III}(dto)_3]$(dto = $C_2O_2S_2$), and have investigated its physical properties[3,4]. In this paper, we report and discuss a new type of phase transition coupled with spin and charge for $(n\text{-}C_nH_{2n+1})_4N[Fe^{II}Fe^{III}(dto)_3]$(N = 3,4) around 120 K, where the charge transfer between the Fe^{II} and Fe^{III} sites occurs reversibly.

EXPERIMENTAL RESULTS AND DISCUSSION

$(n\text{-}C_nH_{2n+1})_4N[Fe^{II}Fe^{III}(dto)_3]$ was synthesized in the similar way to prepare $(n\text{-}C_3H_7)_4N\ [M^{II}Cr^{III}(dto)_3]$(M = Fe, Co, Ni, Zn)[5]. A solution of $KBa[Fe(dto)_3]\cdot 6H_2O$ in a methanol-water mixture was stirred. To this, a solution of $FeCl_2\cdot 4H_2O$ and $(n\text{-}C_nH_{2n+1})_4NBr$ in a methanol-water mixture was added. In this way, $(n\text{-}C_nH_{2n+1})_4N[Fe^{II}Fe^{III}(dto)_3]$ was obtained as black colored precipitate.

$(n\text{-}C_nH_{2n+1})_4N[Fe^{II}Fe^{III}(dto)_3]$ has a two-dimensional network structure with an alternating array of Fe^{II} and Fe^{III} atoms through dto bridges, which is strongly supported by the structural analysis of $(n\text{-}C_3H_7)_4N[Co^{II}Fe^{III}(dto)_3]$[6]. The two-dimensional network structure of $[Co^{II}Fe^{III}(dto)_3]_\infty$ in $(n\text{-}C_3H_7)_4N$ $[Co^{II}Fe^{III}(dto)_3]$ is shown in Figure 1. The X-ray powder diffraction patterns show $(n\text{-}C_nH_{2n+1})_4N$ $[Fe^{II}Fe^{III}(dto)_3]$ and $(n\text{-}C_3H_7)_4N$ $[Co^{II}Fe^{III}(dto)_3]$ to be isomorphous.

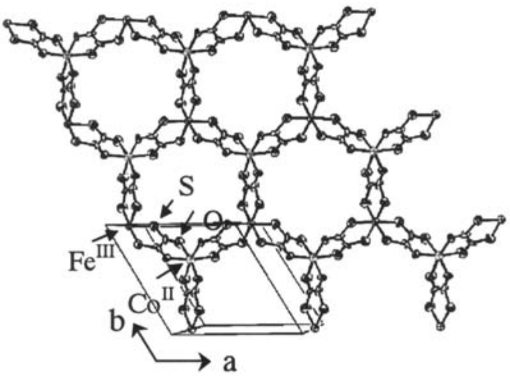

$(C_3H_7)_4N[Co^{II}Fe^{III}(dto)_3]$ R=0.917

FIGURE 1 Network structure of $[Co^{II}Fe^{III}(dto)_3]_\infty$in $(n\text{-}C_3H_7)_4N$ $[Co^{II}Fe^{III}(dto)_3]$.

Figures 2(a) and 2(b) show the ^{57}Fe Mössbauer spectra of $(n\text{-}C_3H_7)_4N[Fe^{II}Fe^{III}(dto)_3]$ at 200 K and 77 K, respectively. At 200 K, the spectrum with two branches at 0.16 mm/s and 1.86 mm/s can be assigned to that for the Fe^{II} site coordinated by six O atoms. As shown in Table I, the isomer shift (*IS*) and the quadrupole splitting (*QS*) of the ^{57}Fe Mössbauer spectrum with two branches at 0.16 mm/s and 1.86 mm/s are quite similar to those of the ^{57}Fe Mössbauer spectrum for the $Fe^{II}(S = 2)$ in $(n\text{-}C_4H_9)_4N[Fe^{II}Cr^{III}(ox)_3]$[7], where the Fe^{II} site is coordinated by six O atoms. The spectrum with single peak at 0.48 mm/s can be assigned to that for the Fe^{III} site coordinated by six S atoms. The *IS* and *QS* of the ^{57}Fe Mössbauer spectrum with single peak at 0.48 mm/s are quite similar to those of the ^{57}Fe Mössbauer spectrum for the $Fe^{III}(S = 1/2)$ in $KBa[Fe^{III}(dto)_3]$, where the Fe^{III} is coordinated by six S atoms[8]. As shown in Figure 2, with decreasing temperature, the line profile of ^{57}Fe Mössbauer spectra remarkably changes between 200 K and 77 K. At 77 K, the intensity of the spectrum corresponding to the Fe^{II} site decreases by 80 % and new lines appears at about 0.2 mm/s and 1.0 mm/s, which implies a drastic change in the Fe electronic states of (n-C_3H_7)$_4$N[Fe^{II}Fe^{III}(dto)$_3$] between 200 K and 77 K.

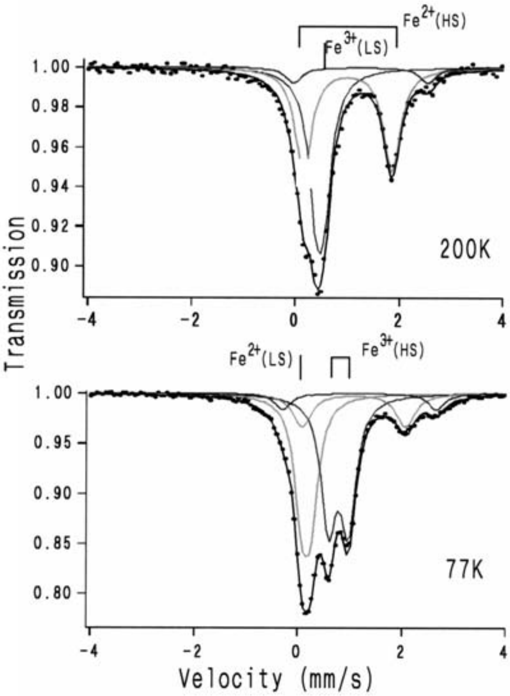

FIGURE 2 ^{57}Fe Mössbauer spectra of (n-C_3H_7)$_4$N[Fe^{II}Fe^{III}(dto)$_3$].

Figure 3(a) shows the ^{57}Fe Mössbauer spectra in the ferromagnetically ordered phase for (n-C_3H_7)$_4$N[Fe^{II}Fe^{III} (dto)$_3$]. The ^{57}Fe Mössbauer spectra at 4.2 K are well resolved and show a superposition of a central peak and a hyperfine split level with six branches. The line profile of ^{57}Fe Mössbauer spectra for (n-C_3H_7)$_4$N[Fe^{II}Fe^{III} (dto)$_3$] in the ferromagnetically ordered phase is quite similar to that of the ^{57}Fe Mössbauer spectra for Prussian blue,

($Fe^{III}_4[Fe^{II}(CN)_6]_3$) below T_c(= 5.5 K)[9], which is shown in Figure 3(b).

In the case of Prussian blue, the spin state of the Fe^{II} site coordinated by six C atoms is the low spin state (S = 0), and that of the

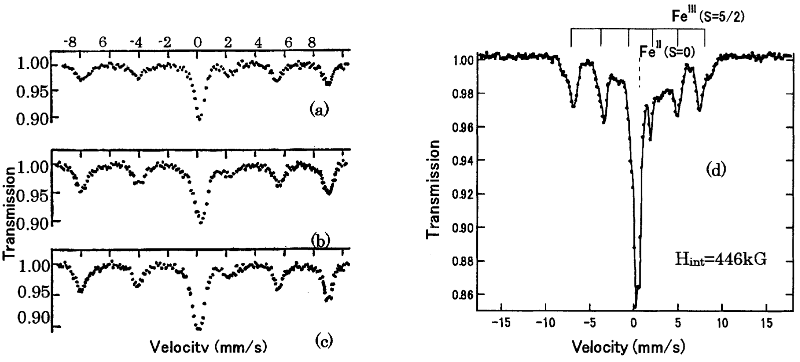

FIGURE 3 ^{57}Fe Mössbauer spectra for Prussian blue at 1.6 K[9] and $(n\text{-}C_3H_7)_4N[Fe^{II}Fe^{III}(dto)_3]$ at 4.2 K. (a) soluble Prussian blue, (b) insoluble Prussian blue, (c) Turnbull's blue, (d) $(n\text{-}C_3H_7)_4N[Fe^{II}Fe^{III}(dto)_3]$.

Fe^{III} site coordinated by N atoms is the high spin state (S = 5/2). The estimated internal magnetic fields for Fe^{II}(S = 0) and Fe^{III}(S = 5/2) in $Fe^{III}_4[Fe^{II}(CN)_6]_3$ at 1.6 K are 0 kG and 540 kG, respectively[9]. Comparing the internal magnetic fields for the Fe^{II} and Fe^{III} sites in $(n\text{-}C_3H_7)_4N[Fe^{II}Fe^{III}(dto)_3]$, the ^{57}Fe Mössbauer spectrum with six split branches induced by the internal magnetic field of 446 kG corresponds to that for the Fe^{III} site with high spin state (S = 5/2), and the central peak without internal magnetic field corresponds to that for the Fe^{II} site with low spin state (S = 0). Taking into account the obtained *IS* and *QS* of the ^{57}Fe Mössbauer spectra for the Fe^{II} and Fe^{III} sites at 4.2 K, the ^{57}Fe Mössbauer spectra of $(n\text{-}C_3H_7)_4N[Fe^{II}Fe^{III}(dto)_3]$ at 77 K can be reproduced as shown in Figure 2(b).

Moreover, in order to prove the charge transfer phase transition at 120 K, we have measured ESR spectra for $(n\text{-}C_3H_7)_4N[Fe^{II}Fe^{III}(dto)_3]$

around 120 K. In the cases of the high-spin state ($^5T_{2g}$) of Fe^{II} and the low-spin state ($^2T_{2g}$) of Fe^{III}, ESR signal can not be observed around 120 K because of rapid spin-lattice relaxation. ESR signal around 120 K is observable only for the high-spin state ($^6A_{1g}$) of Fe^{III}. In fact, as shown in Figure 4, the ESR signal corresponding to the Fe^{III} site with S = 5/2 appears below 120 K, and its intensity becomes strong with decreasing temperature. In the heating process, the ESR signal vanishes above 140 K. The g value of ESR signal at 77 K is 2.10, which is consistent with that of the high-spin state ($^6A_{1g}$) of Fe^{III}. In (n-C_4H_9)$_4$N[Fe^{II}Fe^{III}(dto)$_3$], similar ESR signal corresponding to the Fe^{III} site with S = 5/2 appears below 100 K with decreasing temperature.

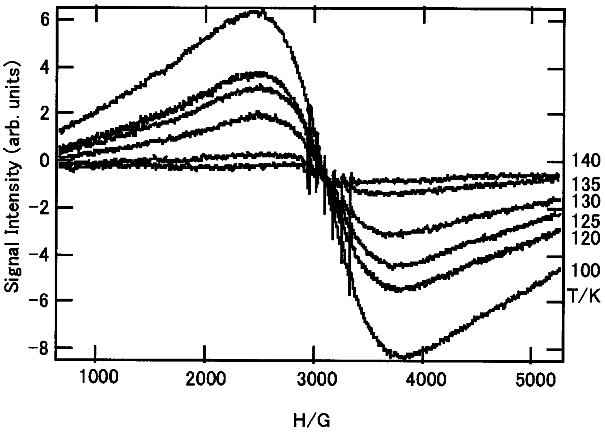

FIGURE 4 ESR signal of (n-C_3H_7)$_4$N[Fe^{II}Fe^{III}(dto)$_3$] around 120 K. Heating process. Hyper fine spectra with six branches around 300 mT correspond to Mn^{2+} in MgO as a marker.

Consequently, it is concluded that (n-C_nH_{2n+1})$_4$N[Fe^{II}Fe^{III}(dto)$_3$](n = 3,4) undergoes a thermally induced charge transfer phase transition coupled with spin transition at 120 K, which is schematically shown in Figure 5. As shown in Figure 5, it is considered that the thermally induced charge transfer transition occurs reversibly between the t_2

orbitals of the Fe^{II} and Fe^{III} sites. The driving force responsible for the charge transfer phase transition would be the difference in spin entropy between the higher and the lower temperature phases. It should be noted that the spin entropy in the higher temperature phase is $R\ln(2 \times 5)$ and that in the lower temperature phase is $R\ln(1 \times 6)$, where R is the gas constant.

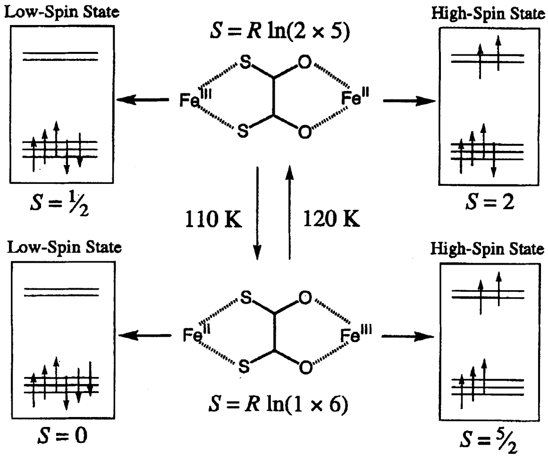

FIGURE 5 Schematic representation of the charge transfer phase transition in $(n\text{-}C_nH_{2n+1})_4N[Fe^{II}Fe^{III}(dto)_3](n = 3, 4)$.

Finally, we discuss the mechanism of ferromagnetic ordering in $(n\text{-}C_nH_{2n+1})_4N[Fe^{II}Fe^{III}(dto)_3]$. As mentioned already, the spin states of the Fe^{II} and Fe^{III} sites in the lower temperature phase are the low-spin state ($S = 0$) and the high spin state ($S = 5/2$), respectively, where the superexchange interaction through the sequence of Fe^{III} – (dto) – Fe^{II} – (dto) – Fe^{III} is considered to be negligibly small. The most plausible mechanism responsible for the ferromagnetic ordering at 6.5 K and 11 K for $(n\text{-}C_3H_7)_4N[Fe^{II}Fe^{III}(dto)_3]$ and $(n\text{-}C_4H_9)_4N[Fe^{II}Fe^{III}(dto)_3]$ is the charge transfer interaction between the Fe^{II} and Fe^{III} sites. In the lower temperature phase of $(n\text{-}C_nH_{2n+1})_4N[Fe^{II}Fe^{III}(dto)_3](n = 3, 4)$, the ground state wave function perturbed by the charge transfer interaction between the Fe^{II} and Fe^{III} sites is expressed as $\Psi = \sqrt{1-\alpha^2}\,\{\phi_i(Fe^{II}(t_2^6))\,\phi_j(Fe^{III}(t_2^3e^2))\} + \alpha\{\phi_i(Fe^{III}(t_2^5))\,\phi_j(Fe^{II}(t_2^4e^2))\}$, where α denotes the degree of the charge transfer interaction. As shown in Figure 5, each Fe^{III} site in the lower temperature phase accepts a t_2 electron with down spin, because the t_2 and e orbitals in the Fe^{III} site are both exactly half occupied. Therefore, the spin configuration between Fe^{II} and Fe^{III} in the virtual state, $\phi_i(Fe^{III}(t_2^5))\,\phi_j(Fe^{II}(t_2^4e^2))$, is ferromagnetically coupled. In this way, the valence delocalization between the Fe^{II} ($S = 0$) and Fe^{III} ($S = 5/2$) sites induces the ferromagnetic ordering in the lower temperature phase of $(n\text{-}C_nH_{2n+1})_4N[Fe^{II}Fe^{III}(dto)_3]$($n = 3, 4$).

Acknowledgement

This work has been supported by a Grant-in-Aid for Science Research from the Ministry of Education, Science, Sports and Culture.

References

[1.] S. Decurtins, P. Gütlich, C.P. Köhler, H. Spiering and A. Hauser, *Chem. Phys. Lett.*, **105**, 1 (1984).

[2.] J. Kröber, E. Codjovi, O. Kahn, F. Grolière and C. Jay, *J. Am. Chem. Soc.*, **115**, 9810 (1993).

[3.] N. Kojima, W. Aoki, M. Seto, Y. Kobayashi and Yu. Maeda, *Synth. Metals*, **121**, 1796 (2001).

[4.] N. Kojima, W. Aoki, M. Itoi, Y. Ono, M. Seto, Y. Kobayashi and Yu. Maeda, *Solid State Commun.*, **120**, 165 (2001).

[5.] H. Ôkawa, M. Mitsumi, M. Ohba, M. Kodera and N. Matsumoto, *Bull. Chem. Soc. Jpn.* **67**. 2139 (1994).

[6.] Y. Ono, M. Ohkubo and N. Kojima, to be published.

[7.] S. Iijima, T. Katsura, H. Tamaki, M. Mitsumi, N. Matsumoto H. Ôkawa, *Mol. Cryst. Liq. Cryst.* **233**, 263 (1993).

[8.] T. Birchall and K.M. Tun, *Inorg. Chem.* **15**, 376 (1976).

[9.] A. Ito, M. Suenaga and K. Ono, *J. Chem. Phys.* **48** (1968) 3597.